Fuel 392 (2025) 134696

Contents lists available at ScienceDirect

Fuel

journal homepage: www.elsevier.com/locate/fuel

Full length article

Bubble growth in composite water/fuel droplets: Effect on timing of their puffing/micro-explosion

Andrey A. Chernov [a], Dmitrii V. Antonov [a,b], Aleksandr N. Pavlenko [a], Tali Bar-Kohany [c,d], Pavel A. Strizhak [a,b], Sergei S. Sazhin [a,b,e,*]

[a] Kutateladze Institute of Thermophysics, Siberian Branch of the Russian Academy of Sciences, 1 Lavrentiev Avenue, Novosibirsk 630090, Russian Federation
[b] Heat and Mass Transfer Laboratory, National Research Tomsk Polytechnic University, 30 Lenin Avenue, Tomsk 634050, Russian Federation
[c] School of Mechanical Engineering, Tel-Aviv University, Tel-Aviv 6997801, Israel
[d] Department of Mechanical Engineering, Nuclear Engineering Research of the Negev, Israel
[e] Advanced Engineering Centre, School of Architecture, Technology and Engineering, University of Brighton, Brighton, BN2 4GJ, UK

ARTICLE INFO

Keywords:
Bubble growth
Composite droplets
Puffing/micro-explosion
Mathematical model
Experimental observations

ABSTRACT

The existing models of bubble growth are reviewed with a view to their possible application to the study of puffing/micro-explosion in composite water/fuel droplets. A simplified version of the Chernov et al. model in the limit of Ja ≫ 1 is demonstrated to be the most suitable for this from the point of view of its simplicity and accuracy. This model is applied to the analysis of timing of puffing/micro-explosion in composite water/n-dodecane droplets placed in air at temperatures varying from 500 to 1000 K. The times to puffing/micro-explosion and bubble growth times for these droplets were obtained based on experiments performed at the National Research Tomsk Polytechnic University. The bubble growth times predicted by this model are shown to be reasonably close to the experimental results. Also the values of these times are very close to those predicted by the direct numerical solution of the underlying equations.

1. Introduction

Much attention has recently focused on the investigation of puffing (swelling of droplets and their break-up into smaller droplets) and micro-explosion (almost instant formation of a cloud of very small child droplets) in composite droplets [1,2]. These phenomena are triggered when the temperature at the interface between two liquids inside the droplet reaches the nucleation temperature of the most volatile liquid (water in most cases) [3].

Puffing and micro-explosion lead to the intensification of the evaporation process due to rapid increase in the area of the liquid/gas interface [4], reduction in NO_x and SO_x emissions by up to 20% [5,6], and fuel consumption by up to 2% [7,8].

Various approaches have been developed to clarify specific features of the phenomena starting with Direct Numerical Simulation (DNS) [9,10] and ending with approaches that use simple models [11,12]. The latter are expected to be complementary to DNS models, focusing on the underlying physics of the processes.

A model originally described in [11,12] assumes that a spherical water sub-droplet is located in the centre of a spherical fuel droplet, heated by convection and radiation. The assumption of the spherical symmetry of the process turned out not to be critical for many practical engineering applications [13,14]. This model assumes that puffing and micro-explosion start at the same time, as they are initiated when the water-fuel interface temperature reaches the water nucleation temperature [11,15].

The latter assumption follows from an implicit assumption that bubble growth, leading to puffing and micro-explosion, is infinitely fast. The effect of finite bubble growth rate on the timing of these processes has been investigated by several authors including [2,16,17], using various models of bubble growth. Although all these papers made important contributions to our understanding of the problem, their applicability to the investigation of puffing and micro-explosion in composite droplets in practical engineering applications turned out to be limited. All of these papers overlooked important developments in bubble growth models described in [18]. Also, the experimental validations of the bubble growth models were limited. These two issues will be addressed in our investigation of the problem, the results of which are presented in this paper.

* Corresponding author at: Advanced Engineering Centre, School of Architecture, Technology and Engineering, University of Brighton, Brighton, BN2 4GJ, UK.

E-mail address: S.Sazhin@brighton.ac.uk (S.S. Sazhin).

https://doi.org/10.1016/j.fuel.2025.134696
Received 6 August 2024; Received in revised form 17 January 2025; Accepted 10 February 2025
Available online 3 March 2025

Nomenclature

a	thermal diffusivity [m^2/s]
A	parameter introduced in Eq. (11) [m/s]
B	parameter introduced in Eq. (11) [$m/s^{1/2}$]
c	specific heat capacity [J/(kg K)]
f	function of the Jakob number introduced in Eq. (5) [-]
Fo	Fourier number
j	mass flux [$kg/(m^2s)$]
Ja	Jakob number [-]
k	thermal conductivity [W/(m K)]
Ku	Kutateladze number [-]
$\mathcal{L}$	specific heat of evaporation [J/kg]
M_v	molar mass of the vapour [kg/mole]
$\bar{M}$	parameter introduced in Eq. (13) [-]
p	pressure [Pa]
r	radial coordinate [m]
R	bubble radius [m]
R_g	gas constant [J/(kg K)]
t	time [s]
t_0	characteristic time of bubble growth $(a_l\rho_l/\Delta p^i)$ [s]
t^*	characteristic time to reach the thermal stage [s]
T	temperature [K]
v	velocity [m/s]
V	volume [m^3]
Y	mass fraction [-]

Greek symbols

α	parameter introduced in Eq. (28) [-]
$\tilde{\alpha}$	parameter introduced in Eq. (13) [s^{-1}]
β	parameter introduced in Eq. (28) [-]
β^f	parameter introduced in Eq. (33) [-]
$\bar{\beta}$	parameter introduced in Eq. (12) [-]
ζ	accommodation coefficient [-]
Θ	dimensionless temperature introduced in Eq. (28) [-]
μ	dynamic viscosity [kg/(m s)]
Π	dimensionless pressure introduced in Eq. (31) [-]
ρ	density [kg/m^3]
σ	surface tension [N/m]
τ	characteristic time [s]
Υ	parameter introduced in Eq. (32) [-]
χ	$r/R(t)$ [-]
ψ	function introduced in Eq. (10) [-]

Hebrew symbols

א	parameter introduced in Eq. (8) [-]
ב	parameter introduced in Eq. (11) [-]
ג	parameter introduced in Eq. (13) [-]
ך	parameter introduced in Eq. (30) [-]

Subscripts

br	droplet break-up
cr	critical
d	droplet
F	fuel
g	gas
gr	bubble growth
l	liquid
N	nucleation
R	interfacial boundary
v	vapour
w	water
0	initial or characteristic value

Superscripts

f	final
i	initial
s	saturated
+	normalised parameters introduced in Eq. (11)

The process of bubble growth preceding puffing/micro-explosions has been extensively studied experimentally. Among the most recent and relevant papers [19,20] are worthy of mention. To the best of our knowledge, however, in all these studies, the initial and boundary conditions were not carefully specified, which makes it difficult to use data presented in these papers for model validation. This is one of the issues to be addressed in the new paper.

Studies of the results of a series of experimental and theoretical investigations (e.g. [21,22]) showed that when certain super-heats of a liquid are achieved during intensive evaporation, the interfacial surface of a rapidly growing vapour bubble loses stability, which leads to the development of the so-called self-sustaining evaporation front. The investigation of this phenomenon, however, is beyond the scope of the current paper.

The aim of this paper is to revisit the problem of the effect of bubble growth on timing of puffing and micro-explosion, specifically focusing on the models which have not been applied to analyses of these phenomena and the range of applicability of these models. The analysis will focus on bubbles filled with water vapour as one of the most important cases for engineering applications, although it can be generalised to any other vapour.

Section 2 focuses on the critical analysis of the most important approaches to modelling bubble growth suggested so far. Based on the results presented in Section 2, the models most relevant to the investigation of puffing and micro-explosion in various experimental conditions will be selected. Section 3 focuses on the key assumptions of one of these models, which has not been applied to the modelling of droplet puffing/micro-explosion, and the details of its incorporation into the numerical code. The results of applications of the selected models to the analysis of the experimentally observed puffing and micro-explosion phenomena, and bubble growth during this process, are presented in Section 4. The key results of the paper are summarised in Section 5.

2. Models of bubble growth

Analysis of the growth of a vapour bubble is a complex problem requiring a coupled solution of the classical fluid dynamic and heat transfer equations. This process is controlled by various fluid dynamic, kinetic, and thermal processes. The dominant process depends on the properties of the two-phase system and can change during bubble growth. Most of the models of this phenomenon, developed so far, have been either over-simplified or based on the Direct Numerical Simulation (DNS) [23,24]. The applicability of DNS models to most engineering problems is limited and most attention has been focused on simplified models. The latter commonly assume that one of the processes is dominant, while the contributions of the remaining processes can be ignored. Obviously, these models have a limited range

of applicability. In this section the most important of these models are briefly reviewed.

The most general classification of widely used bubble growth models was suggested by Labuntsov (see [25] for the details). He referred to these models as 'schemes of growth'.

2.1. Dynamic inertial models

The models of the first group were called 'dynamic inertial' models. These assume that heat supplied to the vapour/liquid interface is unlimited and vapour pressure inside the bubble is maintained at a constant level $p_v = p^s(T^i)$, where $p^s(T^i)$ is saturation pressure at temperature T^i. The latter is assumed to be constant. In this case the rate of bubble growth, controlled by the pressure difference $\Delta p = p_v - p_l$, where p_l is pressure in the liquid away from the interface, can be obtained from the Rayleigh–Plesset (sometimes known as Rayleigh–Lamb) equation [26]:

$$\rho_l\left(R\ddot{R} + \frac{3}{2}\dot{R}^2\right) = p_v - p_l - \frac{2\sigma}{R} - 4\mu_l\frac{\dot{R}}{R}, \tag{1}$$

where R is the bubble radius, and ρ_l and μ_l are liquid density and dynamic viscosity, respectively.

Zanje et al. [27] drew attention to the fact that the assumption of constant saturation pressure may result in an over-prediction of the rate of growth at lower to intermediate Jakob numbers ($\mathrm{Ja} = \rho_l c_l \Delta T/(\rho_v \mathcal{L})$, where ΔT is liquid super-heating, $\mathcal{L}$ specific heat of evaporation, c_l liquid specific heat capacity, ρ_v vapour density).

Ignoring the effects of viscosity, surface tension and interface acceleration, Eq. (1) can be simplified to:

$$\frac{\mathrm{d}R}{\mathrm{d}t} = \sqrt{\frac{2\Delta p}{3\rho_l}}. \tag{2}$$

The dynamic inertial model, described by Eq. (2), is applicable only to the initial stage of bubble growth.

2.2. Dynamic viscous models

The models of the second group were called 'dynamic viscous models'. These assume that the pressure inside a bubble is constant. However, bubble growth in these models is limited by viscous forces, which is typical for highly viscous liquids. The bubble growth in this case is also found from Eq. (1). Ignoring the inertia and surface tension effects, this equation can be simplified to [28]:

$$\frac{\mathrm{d}R}{\mathrm{d}t} = \frac{\Delta p}{4\mu_l}R. \tag{3}$$

2.3. The energy molecular-kinetic models

In the models of the third group, called 'the energy molecular-kinetic models', an attempt is made to consider the kinetics of phase transformation [29,30]. It is assumed that the process is so quick that there is no time for local thermodynamic equilibrium to be established at the liquid vapour interface (the vapour in the bubble is not saturated). The bubble growth rate in this case is determined by the kinetics of the phase transition described by the Hertz–Knudsen kinetic equation at the interface [31]:

$$j = \zeta\frac{p^s(T_{lR}) - p_v}{\sqrt{2\pi\bar{R}_g T_{lR}}}, \tag{4}$$

where T_{lR} is the interface liquid temperature, j is the mass flux, $\bar{R}_g = R_g/M_v$ is the ratio of the gas constant R_g and molar mass of the vapour M_v, ζ is the accommodation coefficient.

The application of these models is necessary only when modelling highly transient processes, characterised by excessive overheating. The non-equilibrium effects described by these models are expected to be observed only during very short time scales (of the order of μs). These models can be applicable to the analysis of explosive boiling. In this case, considerable super-heat is expected when the dynamic and thermal models cannot provide accurate solutions due to the strong contribution of inter-facial processes (see [32]). Moreover, the assumption of constant pressure inside the bubble can be far from realistic, both during the first stage of explosive boiling, and in some cases in composite droplets. A major limitation of energy molecular-kinetic models is the requirement to accurately determine the accommodation coefficient.

2.4. The energy thermal models

The models of the fourth group are called 'the energy thermal models'. These models assume that the growth of the bubble is controlled solely by the heat supply to the liquid/vapour interface from the outer super-heated layers of the liquid. The rate of this heat supply is determined by the temperature head $\Delta T = T^i - T^s(p_v)$ associated with the initial super-heating of the liquid. This heat is spent on evaporation. The vapour pressure in the bubble and in the ambient liquid is assumed to be the same and equal to p_l. To find the bubble growth rate within the framework of this approach, the thermal conductivity equation, with appropriate boundary conditions, is solved. A detailed analysis of these models can be found in the monograph [33].

The solution of the problem using these models is greatly simplified when the analysis is focused on the process over the long term. In this case, a 'self-similar' stage of bubble growth is expected to be reached. This stage is characterised by the establishment of a quasi-steady state when the bubble radius is expected to be proportional to $\sqrt{t}$ with a proportionality coefficient that is a function of the Jakob number:

$$R = f(\mathrm{Ja})\sqrt{a_l t}. \tag{5}$$

The main focus of this group of models has been on finding the type of functional dependence $f(\mathrm{Ja})$.

One of the pioneering papers focused on the development of this group of models was that prepared by Plessett and Zwick [34]. In that paper, the inertial-thermal growth of the bubble was described in terms of an integro-differential equation, which was expanded into a series using a small parameter. Also, it was assumed that liquid temperature changes only in a thin boundary layer near the surface of the bubble. The leading term in the series led to a required asymptotic solution to the problem, which is commonly known as the Plessett–Zwick formula:

$$f(\mathrm{Ja}) = \sqrt{\frac{12}{\pi}}\mathrm{Ja}. \tag{6}$$

A very similar model was proposed by Forster and Zuber in the same year [35]. These authors obtained the following expression:

$$f(\mathrm{Ja}) = \sqrt{\pi}\mathrm{Ja}. \tag{7}$$

Note that both these solutions are applicable for a limited range of Jakob numbers. When deriving these formulae, the authors used a complex multi-stage solution procedure. The bubble growth process was split into separate stages; the terms of the series, obtained as a result of asymptotic expansions, were estimated. Although both these formulae give crude estimates of the rate of bubble growth over long time periods their practical application to solving engineering problems turned out to be limited.

A further step in the development of these models was taken by Birkhoff et al. [36]. These authors looked for a solution to the heat transfer equation in which temperature depended on the dimensionless parameter $\chi = r/R(t)$. This new parameter allowed them to reduce the moving boundary problem to a fixed boundary problem. Their analysis, however, was based on several important assumptions. These include the assumptions that Ja is infinitely large, the vapour density is

negligible, and a thin thermal boundary layer is formed near the surface of the bubble. Using these assumptions, the asymptotic Plessett–Zwick solution was rigorously justified.

Scriven [37] reduced the solution of the problem of bubble growth to the solution of an integral equation:

$$\mathrm{Ja} = \frac{[f(\mathrm{Ja})]^2}{2}\int_1^\infty \chi^{-2}\exp\left\{-\frac{\aleph[f(\mathrm{Ja})]^2}{2}\right\}\mathrm{d}\chi, \tag{8}$$

where

$$\aleph = \frac{(1-\bar{\rho})(1-\chi)}{\chi} + \frac{\chi^2-1}{2},$$

f was introduced earlier.

Eq. (8) is known as the 'Scriven integral'. It contains an implicit expression for $f(\mathrm{Ja})$. Later, Labuntsov and his colleagues proposed a simple approximation of the Scriven integral [33]:

$$f(\mathrm{Ja}) = \sqrt{\frac{12}{\pi}}\mathrm{Ja}\left(1+\frac{1}{2}\left(\frac{\pi}{6\mathrm{Ja}}\right)^{2/3}+\frac{\pi}{6\mathrm{Ja}}\right)^{1/2}. \tag{9}$$

In the limit $\mathrm{Ja} \gg 1$, Expression (9) reduces to the Plessett–Zwick formula (6).

Another solution, valid over a wide range of super-heating, was obtained by Avdeev and Zudin [38]. In the approach used by these authors, it was assumed that the total heat flux can be presented as a superposition of that due to steady-state flow (the effect of fluid movement on bubble growth can be ignored) and transient flow (not only the influence of fluid velocity, but also the permeability of the interfacial boundary was considered). This led to the following expression for the Scriven integral, valid up to the vicinity of the spinodal temperature:

$$f(\mathrm{Ja}) = \sqrt{\frac{3}{\pi}}\mathrm{Ja}\psi + \sqrt{\frac{3}{\pi}(\mathrm{Ja}\psi)^2 + 2\mathrm{Ja}}, \tag{10}$$

where

$$\psi = 1+\sqrt{\frac{\pi}{2}}\left(\frac{1}{1-\frac{c_l\Delta T}{\mathcal{L}}}-1\right)$$

is the correction considering the permeability of the interface.

2.5. Hybrid models

Although the energy thermal models have been widely used in engineering applications, their range of applicability is rather limited as they do not consider the initial and transient stages of the process. During the latter stage, vapour pressure in the bubble approaches the ambient liquid pressure. The assumptions on which these models are based lead to the prediction of infinitely fast initial bubble growth ($\dot{R} \sim 1/\sqrt{t}$), which is physically impossible. This prompted the development of hybrid models that consider both dynamic and thermal effects. This, however, led to the need to consider the time dependence of both vapour pressure in the bubble and the interface temperature, which resulted in a considerable complication of the problem.

Mikic et al. [39] were one of the first teams to attempt to describe all stages of bubble growth. In order to do this, they had to make several important assumptions. The contributions of viscous friction and surface tension were ignored. A linear approximation of the Clapeyron–Clausius equation was used to formulate the pressure difference due to liquid super-heating in the Rayleigh equation (the Rayleigh–Plesset equation in the limit of the inviscid process). Vapour density in the bubble was considered to be constant during the whole process. Despite these assumptions, this paper remains one of the most cited. The analytical solution presented in this paper

$$R^+ = \frac{2\beth}{3}; \quad R^+ = RA/B^2; \quad t^+ = tA^2/B^2, \tag{11}$$

where

$$\beth = \left(t^+ + 1\right)^{3/2} - \left(t^+\right)^{3/2} - 1; \quad A = \sqrt{\frac{2}{3}\frac{\Delta T\mathcal{L}\rho_v}{T^s(p_l)\rho_l}}; \quad B = \mathrm{Ja}\sqrt{\frac{12}{\pi}a_l},$$

reduces to the Rayleigh and Plessett–Zwick solutions in the limit of short and long times, respectively.

Later, Theophanius and Patel [40] modified the Mikic el al. solution, more correctly describing the density and pressure of saturated vapour in the linear approximation of the Clapeyron–Clausius equation:

$$R^+ = \frac{2}{3\bar{\beta}}\left\{\left(\bar{\beta}^2 t^+ + 1\right)^{3/2} - \left(\bar{\beta}^2 t^+\right)^{3/2} - 1\right\}, \tag{12}$$

where

$$\bar{\beta} = \sqrt{\frac{\mathcal{L}\rho_v(p_l)(T^i - T^s(p_l))}{T^s(p_l)(p^s(T^i) - p_l)}}$$

is the coefficient using the parameters of saturation at the interface and away from the bubble and describes the maximal deviation between the solutions suggested by Theophanius and Patel [40] and Mikic et al. [39]. This deviation increases with an increase in the initial to final vapour density ratio. This implies that this deviation increases with an increase in the degree of super-heat. When $\bar{\beta} = 1$, (12) reduces to (11).

Another modification of the Mikic et al. [39] solution was suggested by Miyatake et al. [41]. In that paper, the contribution of surface tension and the nonlinearity of the dependence of saturation pressure on temperature were considered. Also, a time of inertial growth was introduced to the solution, emphasising the importance of this stage of the process.

Prostperetti and Plesset [42] attempted to find a coupled solution to the equations describing bubble dynamics and thermal conductivity. They obtained a solution (which looks similar to the solution obtained by Mikic et al. [39]):

$$\bar{R} = \frac{2\beth}{\pi^2}\sqrt{\frac{2}{3}}, \quad \bar{R} = \bar{M}^2 R/R^i, \quad \bar{t} = \tilde{\alpha}\bar{M}^2 t, \tag{13}$$

where

$$\beth = \left(\frac{\pi^2}{2}\bar{t}+1\right)^{3/2} - \left(\frac{\pi^2}{2}\bar{t}\right)^{3/2} - 1,$$

$$\tilde{\alpha} = \frac{\left(p_v(T^i) - p_l\right)^{3/2}}{2\sigma\rho_l^{1/2}},$$

$$\bar{M} = \frac{1}{3}\left(\frac{2\sigma a_l}{\pi}\right)^{1/2}\frac{\rho_v(T^i)\mathcal{L}}{k_l}\left(T^i - T^s(p_l)\right)^{-1}\left(\rho_l\left[p_v(T^i) - p_l\right]\right)^{-1/4}.$$

Using methods of numerical analysis, Zanje et al. [27] obtained values for bubble growth rates close to those obtained by Mikic et al. [39] at the thermal stage of bubble growth. Note that the thermal stage of bubble growth is well described by other models summarised in this section. The applicability of this approach to the transitional stage has not been carefully investigated. Bar-Kohany et al. [17] presented the results of detailed comparisons of bubble growth predicted by Zanje et al. [27] and Mikic et al. [39] which confirmed the similarity of these predictions for the thermal stage of bubble growth.

Chernov et al. [18] presented another hybrid model for bubble growth in a super-heated liquid, considering both thermal and dynamic effects. Their model was based on classical momentum and heat transfer equations taking into account the evaporation process at the gas–liquid interface. A semi-analytical solution to the problem was found, assuming the existence of a quasi-stationary state for the bubble growth process. This solution is applicable at all stages of the process for a wide range of Jakob numbers (see Appendix for the details). In this approach, the initial boundary value problem, considering a moving boundary, is reduced to a system of relatively straightforward ordinary first-order differential equations. It was shown that in a long time limit the solution becomes self-similar. The resulting asymptotics coincide with the Scriven solution, which, in turn, reduces to the Plessett–Zwick solution at large Jakob numbers. Similar approaches were used in the past to describe the bubble growth in a super-saturated solution and a crystalline nucleus in a super-cooled melt [28,43]. In this paper, the applicability of the model suggested by Chernov et al. [18] to the

analysis of bubble growth at the initial stage of puffing/micro-explosion in composite droplets is carefully studied. The predictions of this model will be compared with the results predicted by the previously used models suggested by Mikic et al. [39] and Zanje et al. [27].

3. Modelling of bubble growth preceding puffing and micro-explosion

As demonstrated in Section 2, hybrid models appear to be the most suitable for the analysis of bubble growth during the initial stage of puffing/micro-explosion events. The latter process is characterised by a wide range of parameters leading to a wide range of Jakob numbers, although for those cases that are most important to engineering applications this number can be assumed to be much greater than 1.

Note that the conditions under which bubble growth occurs within the thermal growth model are achieved at infinitely long times (the thermal growth stage is asymptotic). In this case, an exact solution and a solution obtained by the thermal model are close. This condition, however, is not satisfied in many practical engineering applications. As follows from the analysis presented in [18], typical times when the water vapour bubble growth τ_{gr} reaches the thermal stage of growth are expected to be in the range $\tau_{gr} \gtrsim \left(10^7 - 10^8\right) \cdot t_0$, where $t_0 = a_l \rho_l / \Delta p^i$. Note that $a_l \rho_l / \Delta p^i$ is the only combination of parameters leading to the dimension of time. Thus, t_0 can be considered a characteristic time of the exponential stage of the process.

Times τ_{gr} can be either much less than the typical times for the entire process (in this case, the thermal growth model is applicable), or comparable, or even much longer than these times. In the latter case, the thermal growth model is not applicable, which makes it necessary to develop more complex models to describe bubble growth dynamics. The low limit of τ_{gr} was obtained based on the numerical results for water, and is rather crude [18].

Our analysis will focus mainly on the model suggested by Chernov et al. [18] (see Appendix for the details). This model assumes that a bubble grows due to the 'enthalpy of super-heating' accumulated at the induction stage. Heat spent on the phase transition is stored in the fuel, due to the fact that the mass fraction of water in the composite droplet is small.

An assumption that heat is supplied to the bubble homogeneously from all directions (a spherically symmetric problem is considered) was made. In other words, the bubble growth was assumed to take place in a homogeneous medium with average characteristics. This assumption is valid if the thermal boundary layer around a growing bubble does not reach the droplet surface.

Average super-heating of liquid fuel at the start of nucleation is inferred from the following relationship (it is assumed that the temperature distribution inside the droplet is known):

$$\left\langle \Delta T^i \right\rangle = \frac{\int_{V^i} \left\{ \rho_W c_W \Delta T_W Y_W + \rho_F c_F \Delta T_F (1 - Y_W) \right\} \mathrm{d}V}{\left\{ \rho_W c_W Y_W + \rho_F c_F (1 - Y_W) \right\} V^i}, \tag{14}$$

where Y_W is the mass fraction of water in the droplet; V^i is the initial droplet volume; subscripts 'W' and 'F' indicate water and fuel, respectively; ΔT_W (ΔT_F) is the super-heating of water (liquid fuel) relative to the saturation temperature of the water (difference between the current temperature of water (liquid fuel) and boiling temperature of water). Integration is carried out over the droplet volume. The temperature dependence of liquid thermophysical properties is ignored.

Note that in the cases where nucleation is likely to occur at the interface, it might be more appropriate to consider super-heating at this interface (e.g. interface between the fuel shell and the water inner sub-droplet in a composite droplet) rather than the average super-heating. This approach, however, would require a rigorous numerical solution of a 3D problem, which is not the focus of this paper.

The application of the model starts with estimation of the Jakob number based on the average super-heating, the characteristic time of bubble growth $t_0 = a_l \rho_l / \Delta p^i$, and the characteristic time when the thermal stage is reached, $t^* \approx \left(10^7 - 10^8\right) \cdot t_0$. If $\tau_{gr} < t^*$ then transient bubble growth needs to be considered. In this case, the model suggested by Chernov et al. [18] should be used (see Appendix). If $\tau_{gr} \gtrsim t^*$ then the growing bubble has time to reach the thermal stage. In this case, the solutions obtained using the energy thermal model lead to a simple 'engineering' formula

$$R = \sqrt{2 \beta^f a_l t}, \tag{15}$$

where β^f is the coefficient that is dependent on Ja (see the Appendix for the details).

For $\mathrm{Ja} \gg 1$, which is applicable to most engineering applications,

$$\beta^f \approx (6/\pi)(\mathrm{Ja} + 4/9)^2. \tag{16}$$

Note that times when Formula (15) is applicable may not be achieved in all applications. In this case R can be proportional to t^n where $n \neq 1/2$ [44,45].

Assuming that the bubble originates in the droplet centre, and puffing/micro-explosion starts when R becomes equal to $R_{d,\max} = R_{d0}$, where R_{d0} is the initial droplet radius, the time attributed to bubble growth (τ_{gr}) is estimated as:

$$\tau_{gr} = R_{d0}^2 / (2 \beta^f a_l). \tag{17}$$

Note that the value of $R_{d,\max} = R_{d0}$ is close to the thickness of the fuel shell in the model considered in [17] in which $R_{d,\max} = 2R_{d0}$ for a volume fraction of water equal to 0.1. Ignoring a small difference in the densities of water and fuel, this thickness is estimated as:

$$R_{d,\max} = 2R_{d0} - 2R_{w0} = 2R_{d0}\left(1 - Y_{W0}^{1/3}\right) = 2R_{d0}\left(1 - 0.1^{1/3}\right) = 1.07 R_{d0}. \tag{18}$$

Thus, the result presented by [17], based on the models by Mikic et al. [39] and Zanje et al. [27], who obtained the best agreement between the experimental and modelling results for $R_{d,\max} = 2R_{d0}$, agrees with the one presented in this paper where the best agreement was obtained for $R_{d,\max} = R_{d0}$. Our results are based on the assumption that the bubble originates in the droplet centre and grows until it reaches the droplet surface, while [17] considered a bubble originating at the water/fuel interface and also growing until it reached the surface of the droplet (see Expression (27) of [17]). As follows from (18), both distances can be close.

The time to droplet break-up (τ_{br}), in our model is estimated as [17]:

$$\tau_{br} = \tau_N + \tau_{gr}, \tag{19}$$

where τ_N is the droplet heating time (time taken to heat the fuel/water interface from the initial to the water nucleation temperature).

Note that the estimation of the characteristic time of droplet heating as $\tau_N \approx R_{d0}^2 / a_l$ leads to the expression

$$\tau_{gr} / \tau_N \approx (2\beta^f)^{-1}. \tag{20}$$

As follows from (20) and (16), the time taken for the bubble to grow is comparable to τ_N when $\mathrm{Ja} \sim 1$, and much shorter than τ_N when $\mathrm{Ja} \gg 1$.

This simplified version of the model presented in [18] was verified using the results of direct numerical solution of the underlying equations (Eqs. (21) and (22) in the Appendix) with the appropriate boundary and initial conditions. COMSOL Multiphysics's Moving Geometry dynamic geometry adaptation was used. Calculations were performed on an Intel(R) Xeon(R) CPU E5-2697 v3 @ 2.60 GHz with two processors, and using 128 GB of installed RAM. The typical calculation time for the direct numerical solution was between 1 and 5 min.

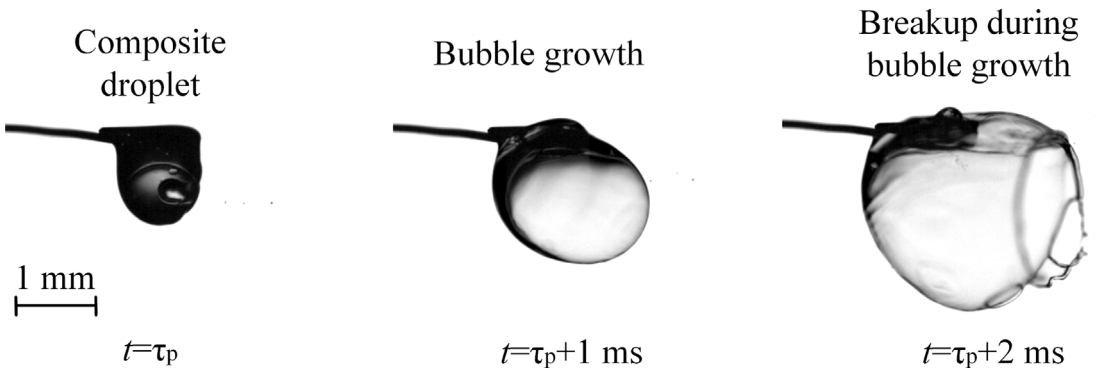

Fig. 1. Experimental observations of bubble growth dynamics in a composite droplet ($R_{d0} = 0.5 \pm 0.05$ mm) in gas at temperature $T_g = 1000 \pm 10$ K; τ_p is the time instant when the droplet is placed into the chamber.

4. Times to puffing/micro-explosion: experiments versus modelling

There has been much uncertainty in identifying the contribution of bubble growth time (τ_{gr}) to the time to puffing/micro-explosions in composite water/fuel droplets (τ_{br}). In the simplest models of the latter phenomenon the contribution of τ_{gr} to τ_{br} was ignored altogether and it was assumed that the latter time can be identified with τ_N (e.g. [11]). Earlier approaches to investigate the contribution of bubble growth to τ_{br} of composite droplets were reviewed by Bar-Kohany et al. [17]. In that paper the bubble growth time predictions of two models, described by Mikic et al. [39] and Zanje et al. [27], were compared with the results of experimental observations of these times performed at the National Research Tomsk Polytechnic University. The results presented in that paper were inconclusive. The predictions of the less detailed model described by Mikic et al. [39] were closer to the experimental results than those predicted by a more accurate model described by Zanje et al. [27]. In both cases, however, the bubble growth times were more than an order of magnitude less than τ_N. This justified the applicability of the model presented in [11] where the contribution of the bubble growth time to time to puffing/micro-explosion was ignored altogether.

Typical images of bubble growth dynamics in a composite droplet ($R_{d0} = 0.5 \pm 0.05$ mm) in a gas at temperature $T_g = 1000 \pm 10$ K are presented in Fig. 1. As follows from this figure, the size of the bubble can exceed the size of the original composite droplet by several times, in agreement with the earlier results [46–48]. It is not clear, however, how this can be considered when modelling the process. As mentioned earlier, in our analysis it was assumed that the bubble grows from the droplet centre until it reaches the original droplet surface, at which point droplet puffing/micro-explosion takes place.

In experiments, three typical practical scenarios have been observed: (1) the bubble originates in the centre of the water sub-droplet; (2) the bubble originates in the water sub-droplet but away from its centre; (3) the bubble originates at the water/fuel interface. Scenarios 1 and 2 are typical for high heating rates (more than 10^6 K/s) [17] of droplets with diameters of less than 10 μm in internal combustion engines [49,50]. Scenario 3 is typical for low heating rates (less than 10^4 K/s) of droplets with diameters of more than 100 μm in marine diesel engines [51,52] and fire extinguishers [53–55]. The analysis of this process is beyond the scope of this paper. As follows from the experimental studies of bubble dynamics at the Heat and Mass Transfer Laboratory of Tomsk Polytechnic University, typical asymmetry of the bubble origin (Scenario 2) leads to modelling errors of not more than 10% compared to the case of Scenario 1 [56], which is acceptable in most engineering applications. Hence, the focus on Scenario 1 in our analysis.

The following analysis compares the timing of puffing/micro-explosion, using in-house experimental data, including that used in [17], but focuses on the model described in Section 3, alongside the previously considered models by Mikic et al. [39] and Zanje et al. [27]. Times to droplet break-up (τ_{br}) versus ambient temperature, observed experimentally, and droplet heating time (τ_N) and time to droplet break-up ($\tau_{br} = \tau_N + \tau_{gr}$) versus ambient temperature, predicted by the model described in Section 3, are presented in Fig. 2a.

Bubble growth time (τ_{gr}) versus ambient gas temperature observed experimentally, predicted by the model presented in Section 3 and described by Mikic et al. [39] and Zanje et al. [27], and the results inferred from the numerical solution of the underlying equations (Eqs. (21) and (22) with the corresponding initial and boundary conditions), are shown in Fig. 2b. A zoomed version of part of Fig. 2b is shown in Fig. 2c. From Figs. 2b and 2c one can see that the predictions of the model described in [18] are almost indistinguishable from the numerical results, which can be considered a verification of this model.

As follows from Fig. 2a, the predicted droplet heating time (τ_N) and time to droplet break-up (τ_{br}) are very close, especially at ambient temperatures above 600 K. Both these times are close to times to droplet break-up (τ_{br}) observed experimentally. In fact predicted τ_N and τ_{br} cannot be validated separately using our experimental data.

As can be seen in Fig. 2b, the bubble growth time predicted by the model described in Section 3 is longer than that predicted by the models by Mikic et al. [39] and Zanje et al. [27], previously used in [17]. The former time is much closer to experimental results than the times predicted by the other two models.

Higher ambient gas temperatures provides higher driving forces for bubble growth in the form of higher Jakob numbers. For a given composite droplet, and any given break-up criterion (e.g. $R_{d,max} = R_{d0}$), this leads to lower break-up times, as shown by all models, and by the experimental results, as seen in Fig. 2a, and lower bubble growth times, as shown in Fig. 2b. Although these trends are similar in all models, their quantitative predictions are significantly different. These stem from the basic assumptions made by these models. For example, the Mikic et al. [39] model assumes a constant, maximal growth rate during the inertial regime, that precedes the final, heat-transfer controlled regime. This assumption leads to an over-prediction of the growth rate for lower and intermediate Jakob numbers, as pointed out by Zanje et al. [27]. However, the inertial regime is expected to be significant only for relatively small composite droplets ($R_{d0} < 100$ μm, see Figure 12 in [17]). The growth rates predicted by both models tend to coincide towards the end of the final, heat-transfer controlled regime (see Fig. 8 in [17]). During the transition between the two regimes, however, the growth rate predicted by Zanje et al. [27] can exceed that predicted by [39] for certain Jakob numbers. As a result, the growth times predicted by Mikic et al. [39] for larger droplets can be longer than those predicted by Zanje et al. [27], as shown in Fig. 2b. The Chernov et al. [18] model, on the other hand, is based on a coupled solution of the momentum and heat transfer equations, taking into account the evaporation process at the interfacial boundary, without using any

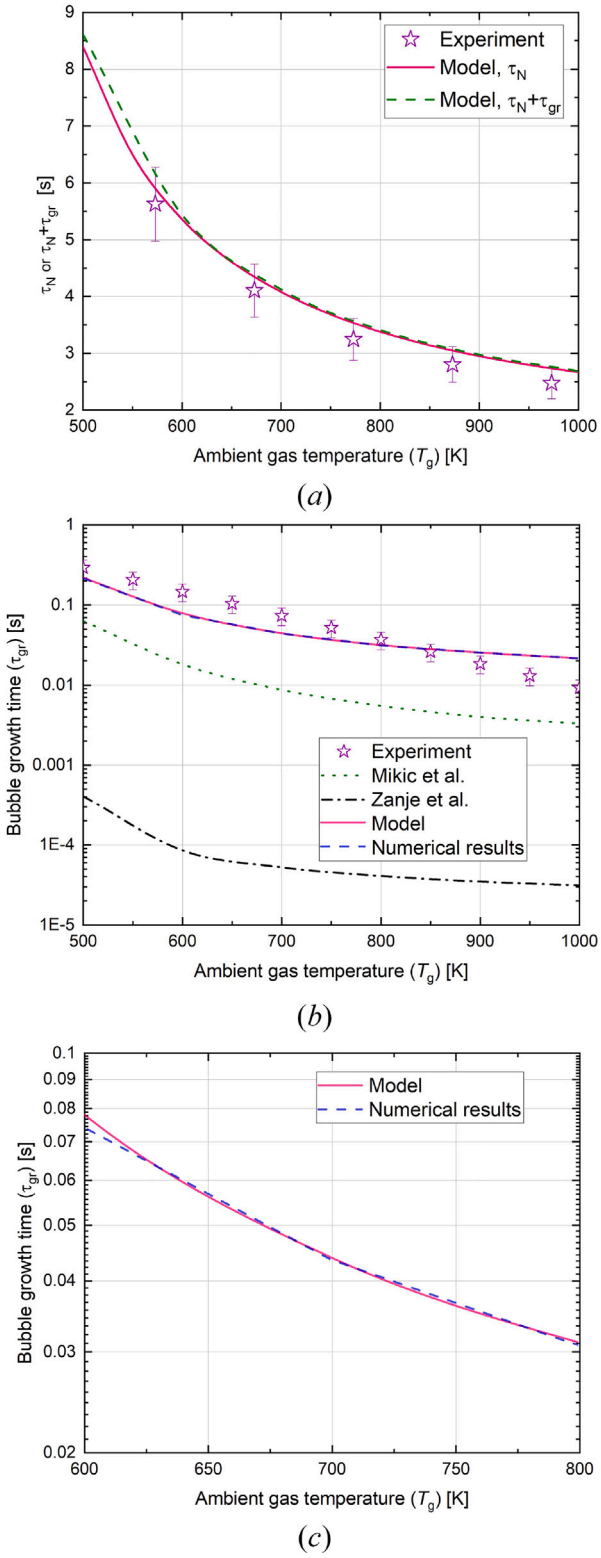

Fig. 2. Times to droplet break-up (τ_{br}) versus ambient temperature, observed experimentally, and droplet heating time (τ_N) and time to droplet break-up (τ_{br}) versus ambient temperature, predicted by the model presented in Section 3 (a); bubble growth time (τ_{gr}) versus ambient gas temperature observed experimentally (Experiment), predicted by the three models: the one described in Section 3 (model) and those described by Mikic et al. [39] and Zanje et al. [27], and inferred from the numerical solution of the underlying equations (Eqs. (21) and (22)) (b); zoomed version of part of Fig. 2b (c); a composite water/n-dodecane droplet with initial radius $R_{d0} = 0.85$ mm and mass fraction of water $Y_W = 0.1$ was used for the analysis.

restrictive assumptions, over a wide range of Jakob numbers. This approach is supported by the close match between the predictions of this model and experimental data.

In the models, the predictions of which are presented in Fig. 2, it was assumed that bubble radius just before droplet break-up does not exceed the initial droplet radius. As mentioned earlier, the actual bubble radius before droplet break-up could exceed the initial droplet radius by up to 5 times [10,47,48,57]. The actual radius of the bubble before fragmentation depends on many parameters in the experiments, including ambient gas temperature, and the properties of the fuel shell and water at different temperatures [17]. Typical values of bubble radius in experiments before puffing/micro-explosion varied from 1.5 to 3 composite droplet initial radii [46–48]. This uncertainty justifies our assumption that the droplet radius is a limiting value for the bubble radius.

The plots of τ_{gr} versus T_g inferred from experimental data (Experiment) and predicted by the model for three values of $R_{d,\max}$ (including the case of $R_{d,\max} = R_{d0}$ used for the plots presented in Fig. 2) are shown in Fig. 3. As expected, the predicted τ_{gr} increases with increasing $R_{d,\max}$, in agreement with the results presented in [17] (see their Figure 18). The best agreement between the experimental and modelling results was achieved for $R_{d,\max} = R_{d0}$, which justifies our initial choice of $R_{d,\max}$.

The assumption that $R_{d,\max} = R_{d0}$ is believed to be acceptable as the first approximation in many technical applications, including those involving internal combustion engines, thermal water treatment, and firefighting [47,58]. It is expected to lead to under-estimation of the time for bubble growth. Another assumption of the model, that the bubble originates in the droplet centre (in most experiments the bubble originates away from the droplet centre), is expected to lead to over-estimation of this time. These two effects are expected to partly compensate for each other. Note the logarithmic scale of the bubble growth time axis in Figs. 2b and 3. This leads to visibly smaller experimental error bars in Figs. 2b and 3 compared with Fig. 2a.

The comparison between the observed and predicted τ_{gr} for three values of the initial droplet radius and the same other parameters as used in Fig. 2 are presented in Fig. 4. As can be seen in Fig. 4, τ_{gr} increased when R_{d0} increased from 0.5 mm to 1 mm. In all cases the predicted τ_{gr} agreed with the observed ones within experimental errors. As the droplet initial radius increased from 0.5 mm to 1 mm, the relative contribution of the bubble growth time to τ_{br} increased from 0.34% to 1.63%.

The plots of normalised bubble radii versus time for three ambient gas temperatures are presented in Fig. 5. As follows from this figure, the rate of growth of R/R_{d0} increases when ambient gas temperature increases, as expected. In all cases, the model predicts results which are reasonably close to experimental measurements.

The maximum deviation between the experimental and modelling results was about 130% at a gas temperature of 1000 K, and the minimal deviation was about 10% for gas temperatures in the range 750 K to 850 K. The main source of measurement errors was in the uncontrolled displacement of the water sub-droplet relative to the fuel shell. The main contributor to the modelling errors was the deviation of the actual bubble radius at which puffing/micro-explosion starts from the bubble radius used in the model. The values of these critical bubble radii depend on several factors, including heating rate, the location of the water sub-droplet relative to the fuel shell, and the presence of impurities in water, amongst others, the effects of which were not carefully investigated in our study.

5. Concluding comments

The earlier suggested models of bubble growth were reviewed with their possible application to the study of puffing and micro-explosion in composite fuel/water droplets. Three models were identified as the most suitable for this application based on the balance between their

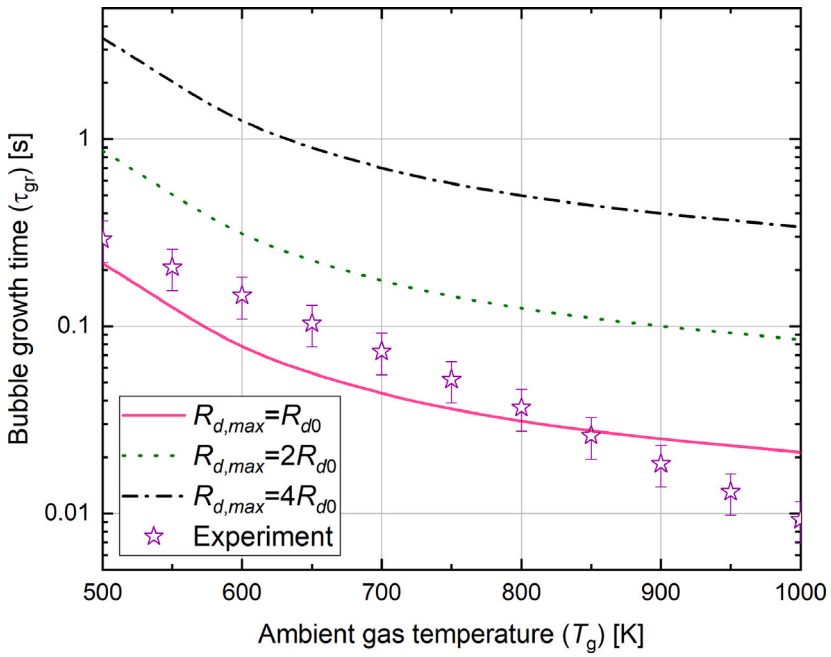

Fig. 3. Bubble growth time (τ_{gr}) versus ambient gas temperature observed experimentally (Experiment) and predicted by the model for three values of the maximal bubble radius before droplet break-up ($R_{d,\max}$); the input parameters are the same as in Fig. 2.

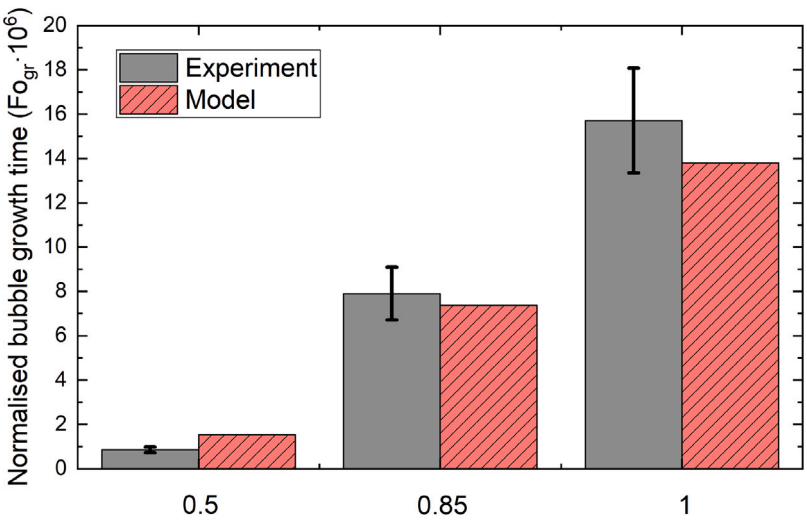

Fig. 4. Normalised times to bubble growth ($Fo_{gr} = a_w\tau_{gr}/R_{d0}^2$) versus droplet normalised initial radii $R_{d0}/R_{d0,\max} = 0.5, 0.85$, and 1, inferred from experimental data (grey) and predicted by the model described in Section 3 (orange); composite water/n-dodecane droplets with mass fraction of water $Y_W = 0.1$ placed in a gas at temperature $T_g = 700$ K were used for the experiments; $a_w = k_w/(c_{pw}\rho_w) = 0.6/(4200\times 1000) \approx 0.14$ mm^2/s; $R_{d0,\max} = 1$ mm. (For interpretation of the references to colour in this figure legend, the reader is referred to the web version of this article.)

accuracy and simplicity. These are the models suggested by Mikic et al. [39], Chernov et al. [18], and Zanje et al. [27]. It was shown that the model suggested by Chernov et al. [18] can be simplified in the limit of large Jakob numbers (Ja ≫ 1), in which case it leads to an explicit expression for bubble growth as a function of time. Assumption Ja ≫ 1 is known to be applicable to the analysis of many practically important engineering processes.

The simplified version of the Chernov et al. [18] model in the limit of Ja ≫ 1 was used for the analysis of bubble growth times and times to puffing/micro-explosion in composite fuel/water droplets. It was assumed that the bubble originates in the centre of the water sub-droplet, and the break-up of the composite droplet takes place when the radius of the bubble becomes equal to the droplet initial radius. This assumption allowed us to derive an explicit formula for the time period of bubble growth (τ_{gr}). Following [17], the time to droplet break-up due to puffing/micro-explosion (τ_{br}) is estimated as the sum of the heating time (time required for the fuel/water interface in the droplet to reach the nucleation temperature of water, τ_N) and τ_{gr}.

The models suggested by Mikic et al. [39], Chernov et al. [18], and Zanje et al. [27] were used for the analysis of puffing/micro-explosion of water/n-dodecane droplets with mass fractions of water equal to 10%, and initial radius equal to 0.85 mm for ambient air temperatures in the range 500 to 1000 K. The times to puffing/micro-explosion for these droplets were obtained based on experiments performed at the National Research Tomsk Polytechnic University. In agreement with the results presented in [17], where the Mikic et al. [39] and Zanje et al. [27] models for bubble growth were used, the bubble growth time inferred from the Chernov et al. model [18] was shown to be much shorter than τ_N and was not expected to have a noticeable effect on the value of τ_{br}.

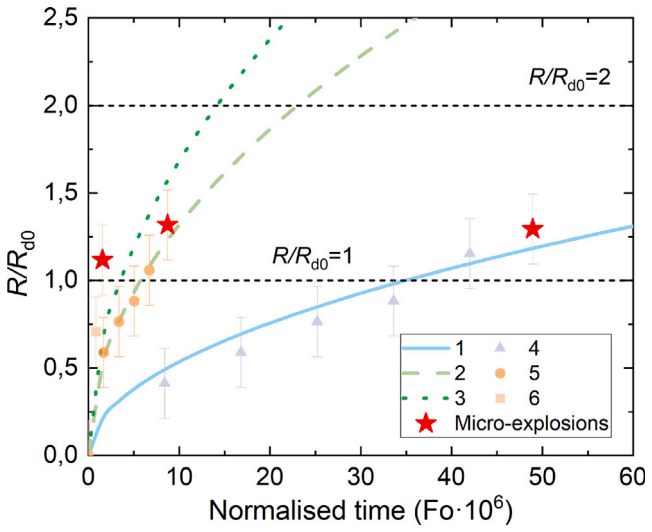

Fig. 5. Normalised bubble radii versus normalised time $Fo_{gr} = a_u t/R_{d0}^2$. (1) Model, T_g = 500 K; (2) Model, T_g = 750 K; (3) Model, T_g = 1000 K; (4) Experiment, T_g = 500 K; (5) Experiment, T_g = 750 K; (6) Experiment, T_g = 1000 K. The input parameters are the same as those used in Fig. 3.

It was shown that the value of τ_{gr} predicted by Chernov et al. [18] is closest to the experimental data when the maximal radius of the vapour bubble ($R_{d,max}$) is assumed equal to the initial droplet radius. Also the values of this time were very close to those inferred from the direct numerical solution of the underlying equations. τ_{gr} was shown to increase with increasing $R_{d,max}$ and increasing initial droplet radius.

It is concluded that, based on the balance of simplicity and accuracy, the model suggested by Chernov et al. [18] can be recommended for the analysis of bubble growth in composite water/fuel droplets.

CRediT authorship contribution statement

Andrey A. Chernov: Writing – review & editing, Writing – original draft, Methodology, Investigation, Formal analysis, Conceptualization. **Dmitrii V. Antonov:** Writing – review & editing, Writing – original draft, Validation, Software, Methodology, Investigation, Formal analysis, Data curation. **Aleksandr N. Pavlenko:** Writing – review & editing, Methodology, Investigation. **Tali Bar-Kohany:** Writing – review & editing, Methodology, Investigation. **Pavel A. Strizhak:** Writing – review & editing, Supervision, Methodology. **Sergei S. Sazhin:** Writing – review & editing, Writing – original draft, Supervision, Project administration, Methodology, Investigation, Formal analysis, Conceptualization.

Declaration of competing interest

The work described has not been published previously and it is not under consideration for publication elsewhere. Its publication is approved by all authors and tacitly or explicitly by the responsible authorities where the work was carried out. If accepted, it will not be published elsewhere in the same form, in English or in any other language, including electronically without the written consent of the copyright-holder.

Acknowledgements

The authors are grateful to Kutateladze Institute of Thermophysics, the Siberian Branch of the Russian Academy of Sciences (State contract) (Section 2), and the Ministry of Science and Higher Education of the Russian Federation (Grant 075-15-2024-620) (Sections 2–5 and Appendix) for their financial support. The research presented in this paper was initiated by the work on a project supported by the Royal Society (UK) (Grant no. IEC 192007).

Appendix. Description of the model suggested in [18]

Let a bubble appear at the initial time instant and start growing in a homogeneously super-heated liquid. The initial bubble radius is assumed to be slightly larger than the critical one $R_{cr} = \frac{2\sigma}{\Delta p^i}$, where Δp^i is the initial value of $\Delta p = p_v - p_l$. The choice of the initial bubble size affects only the duration of the exponential growth stage, which is very short in most cases. The growing bubble very quickly 'forgets' its initial size, and this initial size does not affect most of the process. In practical applications the initial radius is commonly assumed to be 5%–10% larger than R_{cr}, although this is not discussed in the publications.

The equations used for the analysis of this process include well-known classical conservation equations, considering the specifics of the evaporation process. The homogeneous bubble is assumed to be in a state of equilibrium (a local thermodynamic equilibrium is established at the phase transition front). In this case, vapour in the bubble is in a saturated state for the temperature equal to the interface temperature [26].

A modified Rayleigh equation is used to describe bubble dynamics:

$$\frac{1}{R}\frac{\mathrm{d}}{\mathrm{d}t}\left(v_{lR}R^2\right) - \frac{v_{lR}^2}{2} = \frac{p_{lR} - p_l}{\rho_l}, \tag{21}$$

where R is the radius of the bubble; t, p, and ρ are time, pressure, and density, respectively; v_{lR} is the radial liquid velocity at the bubble boundary (in the presence of a phase transition this velocity is not the same as the bubble growth rate $\dot{R}$, these parameters are related as $\rho_l(\dot{R} - v_{lR}) = j$, where j is the vapour flux density). Hereafter, the subscripts l and v refer to liquid and vapour phases, respectively; the superscripts i and f show the initial and final states, respectively; subscript R indicates the interfacial boundary.

Eq. (21) is supplemented by the heat transfer equation in the liquid phase:

$$\frac{\partial\left(\rho_l c_l T_l\right)}{\partial t} + v_l\frac{\partial\left(\rho_l c_l T_l\right)}{\partial r} = \frac{1}{r^2}\frac{\partial}{\partial r}\left(k_l r^2\frac{\partial T_l}{\partial r}\right), \tag{22}$$

where T is temperature, r is the radial coordinate ($r = 0$ refers to the bubble centre),

$$v_l(r) = v_{lR}\left(\frac{R}{r}\right)^2$$

is the radial liquid velocity, inferred from the continuity equation for incompressible fluid, c is the specific heat capacity; all thermophysical properties are assumed to be constant.

The boundary conditions referring to the laws of conservation of mass, momentum and energy are presented as:

$$\rho_v\dot{R} + (1/3)\dot{\rho_v}R = j, \tag{23}$$

$$p_{lR} = p_v + jv_{lR} - \frac{2\sigma}{R} - 4\mu_l\frac{v_{lR}}{R}, \tag{24}$$

$$j\mathcal{L} = k_l\left(\partial T_l/\partial r\right)_{r=R}, \tag{25}$$

where σ is the surface tension; μ is the dynamic viscosity; $\mathcal{L}$ is the specific heat of evaporation; k is the thermal conductivity.

The initial homogeneous liquid temperature is assumed to be greater than the saturation temperature at pressure away from the bubble (p_l): $(T_l)_{t=0} = T^i > T^s(p_l)$. It was assumed that $(T_l)_{r\to\infty} = T^i$ =constant. Local thermodynamic equilibrium is assumed to be valid at the bubble surface: $(T_l)_{r=R} = T^s(p_v)$. Hereafter, the superscript s shows the saturation condition.

The above-mentioned equations are supplemented by the equation of state for the vapour in the bubble, and the dependence of saturated pressure on temperature:

$$\rho_v = \rho_v(p_v, T_v); \tag{26}$$

$$p_v = p^s(T_v) \quad \text{or} \quad T_v = T^s(p_v). \tag{27}$$

The latter can be modelled (Clapeyron–Clausius equation) or empirical dependencies can be applied. Note that the Clapeyron–Clausius equation can be too crude for some applications. In most cases, however, its accuracy is considered to be acceptable.

The system of equations described above can be solved only numerically, even without considering inertial effects, in the general case. An approximate solution to this system was obtained based on the introduction of the new variable $\chi = r/R(t)$. This variable allows us to reduce the boundary value problem to a problem with a fixed boundary (cf. [28]).

Using this new variable, the heat conduction Eq. (22) can be presented as:

$$\frac{R^2}{a_l}\frac{\partial \Theta_l}{\partial t} = \left(-\frac{\alpha}{\chi^2} + \frac{2}{\chi} + \beta\chi\right)\frac{\partial \Theta_l}{\partial \chi} + \frac{\partial^2 \Theta_l}{\partial \chi^2}, \tag{28}$$

where

$$\Theta = \frac{T - T^i}{\Delta T^i}$$

is the dimensionless temperature, $\Delta T^i = T^i - T^s(p_l)$ is the liquid initial super-heating, $\alpha = v_{lR}R/a_l$ and $\beta = \dot{R}R/a_l$ depend on time.

The initial and boundary conditions for (28) are presented as:

$$(\Theta_l)_{t=0} = 0, \quad (\Theta_l)_{\chi=1} = \Theta^s(\bar{\rho}_v), \quad (\Theta_l)_{\chi\to\infty} = 0, \tag{29}$$

where $\bar{\rho}_v = \rho_v/\rho_l$.

We look for a quasi-stationary solution to Eq. (28), with the boundary conditions (29), in the form:

$$\Theta_l(t,\chi) = \Theta^s(\bar{\rho}_v)\frac{\int_0^{1/\chi} \gimel\, d\zeta}{\int_0^1 \gimel\, d\zeta}, \tag{30}$$

where

$$\gimel = \gimel(\zeta) = \exp\left\{-\alpha\zeta - \beta\zeta^{-2}/2\right\}.$$

As follows from numerical estimates, the characteristic time required for reaching a quasi-stationary state is negligible (less by up to two orders of magnitude) compared with the characteristic time of the entire process. Thus, solution (30) can adequately describe the temperature field around the bubble during its growth.

Rearranging Eqs. (21)–(25) and using the temperature profile (30), we obtain the following system of equations:

$$\begin{aligned}
\frac{\mathrm{d}\alpha}{\mathrm{d}t} &= \frac{\Delta p^i}{\rho_l a_l}\Pi^s(\bar{\rho}_v) - \frac{2\sigma}{\rho_l a_l}\frac{1}{R} - \frac{4\mu_l}{\rho_l}\frac{\alpha}{R} - \frac{a_l}{2}\frac{\alpha^2}{R^2},\\
\frac{\mathrm{d}\bar{\rho}_v}{\mathrm{d}t} &= \frac{3a_l\left[\beta\left(1-\bar{\rho}_v\right)-\alpha\right]}{R^2},\\
\frac{\mathrm{d}R}{\mathrm{d}t} &= \frac{a_l\beta}{R},
\end{aligned} \tag{31}$$

where $\Pi = \frac{p_v - p_l}{\Delta p^i}$ is the dimensionless pressure; $\Delta p^i = p^s(T^i) - p_l$ is the initial excess pressure due to overheating of the liquid. The function $\beta = \beta(\alpha, \bar{\rho}_v)$ is implicitly defined by the equation

$$(\beta - \alpha)\int_0^1 Y\, d\zeta = -\mathrm{Ku}^{-1}\,\Theta^s(\bar{\rho}_v), \tag{32}$$

$$Y = \exp\left\{\alpha(1-\zeta) + \beta\left(1-\zeta^{-2}\right)/2\right\},$$

the functions $\Pi^s(\bar{\rho}_v)$ and $\Theta^s(\bar{\rho}_v)$ are inferred from (26) and (27);

$$\mathrm{Ku} = \frac{\mathcal{L}}{c_l \Delta T^i}$$

is the Kutateladze number (the inverse Stefan number), which characterises the initial level of metastability.

This allows us to reduce the problem to the solution of three equations of the type $\mathrm{d}\mathbf{y}/\mathrm{d}t = \mathbf{f}(\mathbf{y})$, where $\mathbf{y} = (\alpha, \bar{\rho}_v, R)$ is the vector function to be found; $\mathbf{f}(\mathbf{y})$ is the right-hand side of System (31).

The vapour pressure in the growing bubble gradually decreases and asymptotically approaches the ambient liquid pressure. At the same time, the vapour density and the temperature of the liquid at the interfacial boundary approach constant values: $\rho_v \to \rho_v^f$; $(\Theta_l)_{\chi=1} \to -1$, where ρ_v^f is the vapour density at pressure p_l.

At this stage of the process, which could be described within the framework of the energy thermal model, the bubble growth is controlled solely by heat transfer to the interfacial boundary, the liquid temperature field becomes stationary, and the functions α and β become constants. The solution of the boundary value problem in this case becomes exact and self-similar:

$$\Theta_l(\chi) = -\frac{\int_0^{1/\chi} \exp\left\{-\beta^f\left[\zeta(1-\bar{\rho}_v^f) + \zeta^{-2}/2\right]\right\} d\zeta}{\int_0^1 \exp\left\{-\beta^f\left[\zeta(1-\bar{\rho}_v^f) + \zeta^{-2}/2\right]\right\} d\zeta};$$

$$R = \sqrt{2\beta^f a_l t}. \tag{33}$$

Note that a similar solution was described by Scriven [37]. The coefficient β^f in Eq. (33) is at this stage a function of only the Jakob number $\mathrm{Ja} = \left(\bar{\rho}_v^f\,\mathrm{Ku}\right)^{-1}$. It can be found from the integral equation (that follows from Eq. (32)):

$$\beta^f \int_0^1 \exp\left\{\beta^f\left[(1-\zeta)(1-\bar{\rho}_v^f) + \left(1-\zeta^{-2}\right)/2\right]\right\} d\zeta = \mathrm{Ja}. \tag{34}$$

For slight super-heating ($\mathrm{Ja} \ll 1$) Eq. (34) has the approximate solution, $\beta^f \approx \mathrm{Ja}$, while for moderate and high super-heating ($\mathrm{Ja} \gtrsim 1$), $\beta^f \approx (6/\pi)(\mathrm{Ja} + 4/9)^2$. The latter coincides with the Plesset-Zwick solution [34] if the additive correction to the Jakob number is not considered. This correction significantly improves the asymptotic approximation. Note that in most practical engineering applications $\mathrm{Ja} \gg 1$.

Data availability

Data will be made available on request.

References

[1] Narasu P, Gutheil E. A new model for puffing and micro-explosion of single titanium(IV) isopropoxide/ p-xylene precursor solution droplets. Int J Heat Mass Transfer 2023;202:123647.

[2] Ray S, Zhang P, Cheng S. Mathematical modeling of puffing and microexplosion in emulsified fuel droplets containing several bubbles: A case study on n-dodecane/water droplet. Fuel 2023;345:128195.

[3] Sazhin SS. Droplets and sprays: Simple models of complex processes. Springer; 2022.

[4] Antonov D, Piskunov M, Strizhak P. Breakup and explosion of droplets of two immiscible fluids and emulsions. Int J Therm Sci 2019;142:30–41. http://dx.doi.org/10.1016/j.ijthermalsci.2019.04.011.

[5] Jeong I, Lee K, Kim J. Characteristics of auto-ignition and micro-explosion behavior of a single droplet of water-in-fuel. J Mech Sci Technol 2008;22:148–56. http://dx.doi.org/10.1007/s12206-007-1018-5.

[6] Javed I, Baek S, Waheed K, Ali G, Cho S. Evaporation characteristics of kerosene droplets with dilute concentrations of ligand-protected aluminum nanoparticles at elevated temperatures. Combust Flame 2013;160:2955–63. http://dx.doi.org/10.1016/j.combustflame.2013.07.007.

[7] Watanabe H, Shoji Y, Yamagaki T, Hayashi J, Akamatsu F, Okazaki K. Secondary atomization and spray flame characteristics of carbonated w/o emulsified fuel. Fuel 2016;182:259–65. http://dx.doi.org/10.1016/j.fuel.2016.05.121.

[8] Suzuki Y, Harada T, Watanabe H, Shoji M, Matsushita Y, Aoki H, et al. Visualization of aggregation process of dispersed water droplets and the effect of aggregation on secondary atomization of emulsified fuel droplets. Proc Combust Inst 2011;33(2):2063–70. http://dx.doi.org/10.1016/j.proci.2010.05.115.

[9] Shinjo J, Xia J, Ganippa L, Megaritis A. Physics of puffing and microexplosion of emulsion fuel droplets. Phys Fluids 2014;278:103302.

[10] Fostiropoulos S, Strotos G, Nikolopoulos N, Gavaises M. Numerical investigation of heavy fuel oil droplet breakup enhancement with water emulsions. Fuel 2020;26:118381.

[11] Sazhin SS, Bar-Kohany T, Nissar Z, Antonov D, Strizhak P, Rybdylova O. A new approach to modelling micro-explosions in composite droplets. Int J Heat Mass Transfer 2020;161:120238.

[12] Sazhin SS, Shchepakina E, Sobolev V, Antonov D, Strizhak P. Puffing/microexplosion in composite multi-component droplets. Int J Heat Mass Transfer 2022;184:122210.

[13] Castanet G, Antonov D, Strizhak P, Sazhin SS. Effects of water subdroplet location on the start of puffing/micro-explosion in composite fuel-water droplets. Int J Heat Mass Transfer 2022;184:122210.

[14] Castanet G, Antonov D, Zubrilin I, Strizhak P, Sazhin SS. Effects of water subdroplet location on the start of puffing/micro-explosion in composite multi-component fuel-water droplets. Fuel 2023;341:127609.

[15] Skripov P, Bar-Kohany T, Antonov D, Strizhak P, Sazhin SS. Approximations for the nucleation temperature of water. Int J Heat Mass Transfer 2023;207:123970.

[16] Fostiropoulos S, Strotos G, Nikolopoulos N, Gavaises M. A simple model for breakup time prediction of water-heavy fuel oil emulsion droplets. Int J Heat Mass Transfer 2021;164:120581.

[17] Bar-Kohany T, Antonov D, Strizhak P, Sazhin SS. Nucleation and bubble growth during puffing and micro-explosions in composite droplets. Fuel 2023;340:126991.

[18] Chernov AA, Pil'nik AA, Vladyko IV, Lezhnin SI. New semi-analytical solution of the problem of vapor bubble growth in superheated liquid. Sci Rep 2020;10(1):16526. http://dx.doi.org/10.1038/s41598-020-73596-x.

[19] Liu Z, Jia M, Liu H, Zhang Y, Li H. Understanding the boiling characteristics of bi-component droplets with improved bubble nucleation and break-up mechanisms. Int J Multiph Flow 2024;179:104918.

[20] Wang J, Zhang Q, Wang X, Xu J. Micro-explosion characteristics and mechanism of multi-component fuel droplet with high volatility differential. Fuel 2023;333(1):126370.

[21] Pavlenko A, Koverda V, Skokov V, Reshetnikov A, Vinogradov A, Surtaev A. Transitional processes dynamics and structures formation for critical regimes of heat and mass transfer at boiling and cavitation of liquids. J Eng Thermophys 2009;18(1):195–224.

[22] Pavlenko A, Koverda V, Reshetnikov A, Surtaev AS, Tsoi A, Mazheiko N, et al. Disintegration of flows of superheated liquid films and jets. J Eng Thermophys 2013;22(3):174–93.

[23] Donne M, Ferranti M. The growth of vapor bubbles in superheated sodium. Int J Heat Mass Transfer 1975;18(4):477–93.

[24] Bhati J, Paruya S. A semi-analytical method for computing the dynamics of bubble growth: The effect of superheat and operating pressure. Ind Eng Chem Res 2018;57(44):15159–71. http://dx.doi.org/10.1021/acs.iecr.8b02231.

[25] Zudin YB. Non-equilibrium evaporation and condensation processes. Springer; 2019.

[26] Nigmatulin RI. Dynamics of multiphase media. Corp, NewYork: Hemisphere Publ; 1990.

[27] Zanje S, Iyer K, Murallidharan JS, Punekar H, Gupta VK. Development of generalized bubble growth model for cavitation and flash boiling. Phys Fluids 2021;33(7):077116. http://dx.doi.org/10.1063/5.0055744.

[28] Chernov AA, Pil'nik AA, Davydov MN, Ermanyuk EV, Pakhomov MA. Gas nucleus growth in high-viscosity liquid under strongly non-equilibrium conditions. Int J Heat Mass Transfer 2018;123:1101–8.

[29] Labuntsov DA, Kryukov AP. Analysis of intensive evaporation and condensation. Int J Heat Mass Transfer 1979;22(7):989–1002.

[30] Pavlov PA. Evaporation of a highly superheated liquid. Int J Heat Mass Transfer 2015;88:203–9.

[31] Zudin YB. Non-equilibrium evaporation and condensation processes. Springer; 2019.

[32] Shusser M, Ytrehus T, Weihs D. Kinetic theory analysis of explosive boiling of a liquid droplet. Fluid Dyn Res 2000;27(6):353.

[33] Avdeev AA. Bubble systems. Springer; 2016.

[34] Plesset MS, Zwick SA. The growth of vapor bubbles in superheated liquids. J Appl Phys 1954;25(4):493–500.

[35] Forster HK, Zuber N. Growth of a vapor bubble in a superheated liquid. J Appl Phys 1954;25(4):474–8.

[36] Birkhoff G, Margulies RS, Horning WA. Spherical bubble growth. Phys Fluids 1958;1(3):201–4.

[37] Scriven LE. On the dynamics of phase growth. Chem Eng Sci 1959;10(1):1–13.

[38] Avdeev AA, Zudin YB. Thermal energy scheme of vapor bubble growth (Universal approximate solution). High Temp 2002;40(2):264–71.

[39] Mikic BB, Rohsenow WM, Griffith P. On bubble growth rates. Int J Heat Mass Transfer 1970;13(4):657–66.

[40] Theofanous T, Patel P. Universal relations for bubble growth. Int J Heat Mass Transfer 1976;19(4):425–9.

[41] Miyatake O, Tanaka I, Lior N. A simple universal equation for bubble growth in pure liquids and binary solutions with a nonvolatile solute. Int J Heat Mass Transfer 1997;40(7):1577–84.

[42] Prosperetti A, Plesset MS. Vapour-bubble growth in a superheated liquid. J Fluid Mech 1978;85(2):349–68.

[43] Chernov AA, Pil'nik AA. Mechanism of growth of a crystalline nucleus in a supercooled melt at large deviations from equilibrium. JETP Lett 2015;102(8):526–9. http://dx.doi.org/10.1134/S0021364015200023.

[44] Siedel S, Cioulachtjian S, Bonjour J. Experimental analysis of bubble growth, departure and interactions during pool boiling on artificial nucleation sites. Exp Therm Fluid Sci 2008;32(8):1504–11.

[45] Lee H, Oh B, Bae S, Kim S. Single bubble growth in saturated pool boiling on a constant wall temperature surface. Int J Multiph Flow 2003;29(12):1857–74.

[46] Antonov D, Fedorenko R, Kuznetsov G, Strizhak P. Modeling the microexplosion of miscible and immiscible liquid droplets. Acta Astronaut 2020;171:69–82.

[47] Antonov D, Kuznetsov G, Fedorenko R, Strizhak P. Ratio of water/fuel concentration in a group of composite droplets on high-temperature heating. Appl Therm Eng 2022;206:118107.

[48] Yi P, Li T, Fu Y, Xie S. Transcritical evaporation and micro-explosion of ethanol-diesel droplets under diesel engine-like conditions. Fuel 2021;284:118892.

[49] Huo M, Lin S, Liu H, Lee C. Study on the spray and combustion characteristics of water-emulsified diesel. Fuel 2014;123:218–29. http://dx.doi.org/10.1016/j.fuel.2013.12.035.

[50] Ismael M, Heikal M, Aziz A, Syah F, Zainal E, Crua C. The effect of fuel injection equipment on the dispersed phase of water-in-diesel emulsions. Appl Energy 2018;222:762–71. http://dx.doi.org/10.1016/j.apenergy.2018.03.070.

[51] Kornienko V, Radchenko R, Radchenko M, Radchenko A, Pavlenko A, Konovalov D. Cooling cyclic air of marine engine with water-fuel emulsion combustion by exhaust heat recovery chiller. Energies 2022;25:4–8. http://dx.doi.org/10.3390/en15010248.

[52] Jiaqiang E, Zhang Z, Chen J, Pham M, Zhao X, Peng Q, et al. Performance and emission evaluation of a marine diesel engine fueled by water biodiesel-diesel emulsion blends with a fuel additive of a cerium oxide nanoparticle. Energy Convers Manage 2018;169:194–205. http://dx.doi.org/10.1016/j.enconman.2018.05.073.

[53] Antonov D, Kovalev D, Shahray M, Fedorenko R. Enhancing the vaporization and secondary atomization of two-liquid droplets for fire suppression. Fire Saf J 2024;146:104155. http://dx.doi.org/10.1016/J.FIRESAF.2024.104155.

[54] Antonov D, Strizhak P. Intensification of vaporization and secondary atomization of droplets of fire-extinguishing liquid composition. Tech Phys Lett 2020;46:122–5. http://dx.doi.org/10.1134/S1063785020020029.

[55] Mahmud H, Thorpe G, Moinuddin K. The behaviour of water-mists in hot air induced by a room fire: effect of the initial size of droplets. Fire 2022;5(4):116. http://dx.doi.org/10.3390/fire5040116.

[56] Shusser M, Weihs D. Explosive boiling of a liquid droplet. Int J Multiph Flow 1999;25:1561–73.

[57] Antonov D, Fedorenko R, Kuznetsov G, Strizhak P. Modeling the micro-explosion of miscible and immiscible liquid droplets. Acta Astronaut 2020;171:69–82.

[58] Antonov D, Fedorenko R, Yanovskiy L, Strizhak P. Physical and mathematical models of micro-explosions: achievements and directions of improvement. Energies 2023;16(16):6034.